

BER Minimized OFDM Systems With Channel Independent Precoders

Yuan-Pei Lin, *Member, IEEE*, and See-May Phoong, *Member, IEEE*

Abstract—We consider the minimization of uncoded bit error rate (BER) for the orthogonal frequency division multiplexing (OFDM) system with an orthogonal precoder. We analyze the BER performance of precoded OFDM systems with zero forcing and minimum mean squared error (MMSE) receivers. In the case of MMSE receivers, we show that for quadrature phase shift keying (QPSK), there exists a class of optimal precoders that are channel independent. Examples of this class include the discrete Fourier transform (DFT) matrix and the Hadamard matrix. When the precoder is the DFT matrix, the resulting optimal transceiver becomes the single carrier system with cyclic prefix (SC-CP) system. We also show that the worst solution corresponds to the conventional OFDM system; the conventional OFDM system has the largest BER. In the case of zero forcing receivers, the design of optimal transceiver depends on signal-to-noise ratio (SNR). For higher SNR, solutions of optimal precoders are the same as those of MMSE receivers.

Index Terms—BER optimal multicarrier, OFDM, precoded OFDM, single carrier.

I. INTRODUCTION

THE DISCRETE Fourier transform (DFT)-based transceiver has found applications in a wide range of transmission channels, either wired [1]–[3] or wireless [4]–[8]. It is typically called discrete multitone (DMT) for wired digital subscriber loop (DSL) applications and orthogonal frequency division multiplexing (OFDM) for wireless local area network (LAN) and broadcasting applications, e.g., digital audio broadcasting [7] and digital video broadcasting [8]. The transmitter and receiver perform, respectively, M -point indiscrete Fourier transform (IDFT) and DFT computation, where M is the number of tones or number of subchannels. At the transmitter side, each block is padded with a cyclic prefix of length L . The number L is chosen to be no smaller than the order of the channel, which is usually assumed to be an FIR filter. The prefix is discarded at the receiver to remove interblock ISI. As a result, a finite impulse response (FIR) channel is converted into M frequency-nonsselective parallel

subchannels. The subchannel gains are the M -point DFT of the channel impulse response.

For wireless transmission, the channel profile is usually not available to the transmitter. The transmitter is typically channel independent, and there is no bit/power allocation. Having a channel-independent transmitter is also a very useful feature for broadcasting applications, where there are many receivers with different transmission paths. In OFDM systems, the channel-dependent part of the transceiver is a set of M scalars at the receiver, and the transmitter is channel independent. In DSL applications, the channel does not vary rapidly. The transmitter has the channel profile, which allows bit and power allocation to be employed. Using bit allocation, the disparity among the subchannel noise variances is exploited in the DMT system for bit rate maximization. The DMT system has been shown to be a very efficient technique in terms of transmission rate for a given probability of error and transmission power.

In the context of transceiver designs for wireless applications, the single carrier system with cyclic prefix (SC-CP) system [9] is also a DFT-based transceiver with a channel independent transmitting matrix, i.e., the identity matrix. A cyclic prefix is also inserted like in the OFDM system. The receiver performs both DFT and IDFT operations. It is demonstrated that the SC-CP system has a very low peak to average power ratio (PAPR). Furthermore, numerical experiments demonstrate that it outperforms the OFDM system for a useful range of bit error rate (BER) [10]. We will see later that the SC-CP system can be viewed as the OFDM system with a DFT precoder. In [11], precoded vector OFDM systems are proposed for combating spectral nulls. When the channel has spectral nulls, the proposed system outperforms the conventional OFDM system. In the precoded vector OFDM scheme, more redundant samples are needed than in the conventional OFDM system. In [12], designs of linear precoding to maximize diversity gain are considered.

Design of more general block transceivers, which are optimal in the sense of minimum transmission power or minimum total noise power, has been of great interest. In [13], general block transceivers, which are not constrained to be DFT matrices, are investigated. For the class of zero-padding transceivers, an optimal solution that minimizes the total output noise variance is given in [13]. The optimal receiver and zero-padding transmitter can be given in terms of an appropriately defined channel matrix and the autocorrelation matrix of the channel noise. Information rate optimized DMT systems are considered in [14] and [15]. In [16], intersymbol interference (ISI)-free block transceivers are considered. Under an optimal bit allocation, optimal transmitters and receivers that minimize transmission power for a given

Manuscript received August 27, 2002; revised February 3, 2003. This work was supported in part by the National Science Council, Taiwan, R.O.C., under Grants NSC 90-2213-E-002-097 and 90-2213-E-009-108, the Ministry of Education, Taiwan, R.O.C., under Grant 89E-FA06-2-4, and the Lee and MTI Center for Networking Research. The associate editor coordinating the review of this paper and approving it for publication was Prof. Nicholas D. Sidiropoulos.

Y.-P. Lin is with the Department Electrical and Control Engineering, National Chiao Tung University, Hsinchu, Taiwan, R.O.C. (e-mail: ypl@cc.nctu.edu.tw). S.-M. Phoong is with the Department of Electrical Engineering and Graduate Institute of Communication Engineering, National Taiwan University, Taipei, Taiwan, R.O.C.

Digital Object Identifier 10.1109/TSP.2003.815391

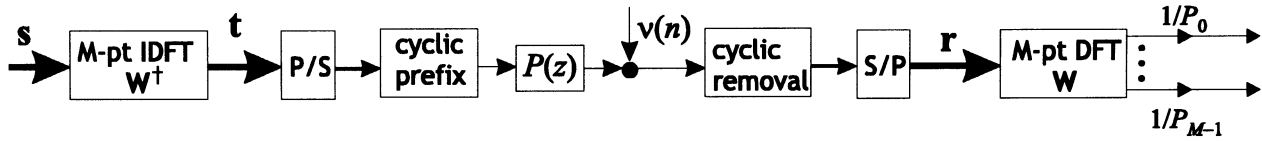


Fig. 1. Block diagram of the OFDM system over a channel $P(z)$ with additive noise $\nu(n)$.

bit rate and probability of error are derived. In all these systems [13]–[16], it is assumed that the transmitter has the channel profile.

Recently, based on the zero-forcing solution given in [13], Ding *et al.*¹ consider a class of optimal precoders in [17], in which a precoder refers to the transmitting matrix. It is assumed in both [13] and [17] that the transmitter has the channel profile. The optimal transmitter that minimizes the output noise variance consists of a unitary matrix, a diagonal power loading matrix, and a second unitary matrix that is arbitrary [13]. The first unitary matrix exposes the eigenmodes of the channel, whereas power loading exploits the eigenmodes to reduce the total noise variance. The second unitary matrix is optimized in [17] to minimize BER. For high SNR, the DFT matrix has been found to be optimal for BPSK modulation. The resulting transmitter is channel dependent.

In this paper, we will consider the minimization of BER for OFDM systems with orthogonal precoders. The underlying system is, in fact, the class of cyclic prefixed block transceivers with orthogonal transmitters. We will address the design of optimal precoders with the assumption that there is no bit and power allocation. Notice that the objective is BER, rather than mean squared error (MSE). In the conventional single-band transmission system, BER is directly tied to mean squared error. For multisubchannel systems like OFDM and SC-CP systems, this is no longer true. In the absence of bit and power allocation, transceivers with the same total noise variance can have different BER performances. This is because different transceiver designs distribute the noise among the subchannels differently. We will consider the design of optimal precoders for zero forcing and for MMSE receivers. In the MMSE case, we show that when the modulation symbols are QPSK, optimal precoders are not unique. In this case, there exists a whole class of channel-independent optimal precoders. Examples of precoders in this class include the DFT matrix and the Hadamard matrix. It turns out that when the precoder is chosen as the DFT matrix, the resulting transceiver becomes the SC-CP system [9]. On the other hand, we also show that the identity matrix is the worst precoder, and the conventional OFDM system has the largest BER. In the case of zero forcing receiver, solutions of optimal precoders are SNR dependent. For higher SNR, there also exists a class of channel-independent optimal precoders. The optimal solutions are the same as those of the MMSE receivers. We will derive the results for QPSK modulations. Generalizations to phase amplitude modulation (PAM), phase shift keying (PSK), and quadrature amplitude modulation (QAM), based on approximated BER from symbol error rate formulae, can be obtained with slight modifications. Some

preliminary results on the zero-forcing case can be found in [23] and [24].

The sections are organized as follows. In Section II, we present the schematic of an OFDM system with an orthogonal precoder. We will state results of the conventional OFDM and the SC-CP systems that will be useful for later discussion. In Section III, we consider zero forcing receivers and derive the optimal precoder for QPSK modulation. Extensions to modulation schemes other than QPSK are given in Section IV. The performance of a precoded OFDM system with an MMSE receiver is analyzed in Section V. Numerical examples of BER performances are given in Section VI. A conclusion is given in Section VII.

A. Notations and Preliminaries

- 1) Boldfaced lower case letters represent vectors, and boldfaced upper case letters are reserved for matrices. The notation \mathbf{A}^\dagger denotes transpose-conjugate of \mathbf{A} .
- 2) The function $E[y]$ denotes the expected value of a random variable y .
- 3) The notation \mathbf{I} is used to represent the $M \times M$ identity matrix.
- 4) The notation \mathbf{W} is used to represent the $M \times M$ unitary DFT matrix given by

$$[\mathbf{W}]_{kn} = \frac{1}{\sqrt{M}} e^{-j(2\pi/M)kn}, \quad \text{for } 0 \leq k, n \leq M-1.$$

II. OFDM TRANSCIVERS WITH ORTHOGONAL PRECODERS

The block diagram of the OFDM system is as shown in Fig. 1. The modulation symbols to be transmitted are first blocked into M by 1 vectors, where M is the number of subchannels. Each input vector \mathbf{s} of modulation symbols is passed through an M by M IDFT matrix, followed by the parallel to serial (P/S) operation and the insertion of redundant samples. The length of redundant samples L is chosen to be no less than the order of the channel $P(z)$ so that inter-block interference can be removed. Usually the redundancy is in the form of a cyclic prefix. At the receiving end the cyclic prefix is discarded. The samples are again blocked into M by 1 vectors for M -point DFT computation. The scalar multipliers $1/P_k$, for $k = 0, 1, \dots, M-1$, are the only channel dependent part of the transceiver design, where P_0, P_1, \dots, P_{M-1} are the M -point DFT of the channel impulse response $p(n)$. In this case, ISI is canceled completely, and the receiver is a zero-forcing receiver.

In this paper, we consider the class of block transceivers with an $M \times M$ orthogonal transmitter, followed by cyclic prefix insertion. This class of system can be viewed as an OFDM system with a unitary precoding matrix \mathbf{T} , as shown in Fig. 2, where \mathbf{T}

¹The authors would like to thank the anonymous reviewers for bringing this reference to our attention.

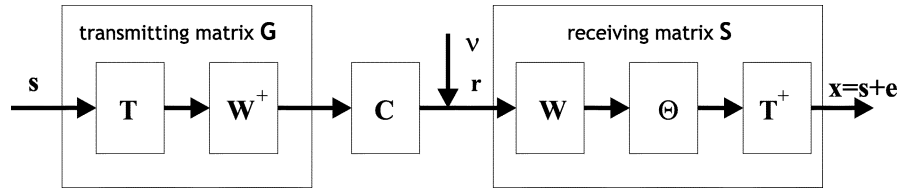
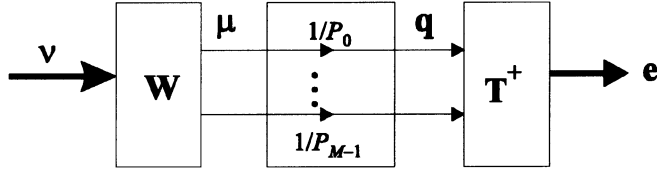

 Fig. 2. OFDM system with a precoder \mathbf{T} .


Fig. 3. Illustration of noise path at a zero-forcing receiver.

is unitary with $\mathbf{T}^\dagger \mathbf{T} = \mathbf{I}$. The resulting block transceiver has a unitary transmitting matrix $\mathbf{G} = \mathbf{W}^\dagger \mathbf{T}$. To have a zero-forcing receiver, \mathbf{T}^\dagger is cascaded to the end of the receiver. The transmitting matrix \mathbf{G} and receiving matrix \mathbf{S} are as shown in Fig. 2. By considering the optimal solution of the precoder \mathbf{T} , we are addressing the problem of designing optimal cyclic-prefixed block transceivers with orthogonal transmitters.

Bit Error Rate: We assume that the channel noise $\nu(n)$ is complex circular AWGN with variance \mathcal{N}_0 . The modulation scheme is QPSK, and modulation symbols $s_k = \pm\sqrt{\mathcal{E}_s/2} \pm j\sqrt{\mathcal{E}_s/2}$ with symbol energy \mathcal{E}_s . Let the receiver output vector \mathbf{x} be as indicated in Fig. 2; then, the output error vector is $\mathbf{e} = \mathbf{x} - \mathbf{s}$. The vector \mathbf{e} comes entirely from the channel noise as the receiver is zero forcing. The noise vector \mathbf{e} can be analyzed by considering the receiver block diagram in Fig. 3. The $M \times 1$ vector $\boldsymbol{\nu}$ consists of a block of size M of the noise process $\nu(n)$. The elements of $\boldsymbol{\nu}$ are uncorrelated Gaussian random variables with variance \mathcal{N}_0 . The elements of $\boldsymbol{\mu} = \mathbf{W}\boldsymbol{\nu}$ continue to be uncorrelated Gaussian random variables with variance \mathcal{N}_0 , due to the unitary property of \mathbf{W} . Therefore, the k th element of the noise vector \mathbf{q} has variance given by $\sigma_{q_k}^2 = \mathcal{N}_0/|P_k|^2$. The output noise \mathbf{e} is related to \mathbf{q} by

$$e_i = \sum_{k=0}^{M-1} t_{k,i}^* q_k$$

where $t_{k,i}$ denotes the (k, i) th element of \mathbf{T} . As q_k are uncorrelated, the i th subchannel noise variance $\sigma^2(i) = \sum_{k=0}^{M-1} |t_{k,i}|^2 \sigma_{q_k}^2$. That is

$$\sigma^2(i) = \mathcal{N}_0 \sum_{k=0}^{M-1} \frac{|t_{k,i}|^2}{|P_k|^2}, \quad \text{for } i = 0, 1, \dots, M-1. \quad (1)$$

The real and imaginary parts of e_i have equal variance. Let $\beta(i) = \mathcal{E}_s/\sigma^2(i)$, which is the SNR of the i th subchannel; then

$$\beta(i) = \frac{\gamma}{\sum_{k=0}^{M-1} \frac{|t_{k,i}|^2}{|P_k|^2}}, \quad \text{where } \gamma = \mathcal{E}_s/\mathcal{N}_0. \quad (2)$$

As \mathbf{T} is unitary, we have $\sum_{i=0}^{M-1} |t_{k,i}|^2 = 1$. Using this fact, we can write the average mean square error (MSE) $\mathcal{E}_{rr} = 1/M \sum_{i=0}^{M-1} \sigma^2(i)$ as

$$\mathcal{E}_{rr} = \frac{\mathcal{N}_0}{M} \sum_{i=0}^{M-1} \frac{1}{|P_i|^2}. \quad (3)$$

The average MSE is independent of \mathbf{T} . All zero-forcing OFDM transceivers with a unitary precoder \mathbf{T} have the same MSE given in (3).

For QPSK modulation, the BER of the i th subchannel is [19]

$$\mathcal{P}_T(i) = Q\left(\sqrt{\frac{\mathcal{E}_s}{\sigma^2(i)}}\right)$$

where $Q(y) = \frac{1}{\sqrt{2\pi}} \int_y^\infty e^{-t^2/2} dt, \quad y \geq 0$.

The average BER is

$$\mathcal{P}_T = \frac{1}{M} \sum_{i=0}^{M-1} Q\left(\sqrt{\frac{\mathcal{E}_s}{\sigma^2(i)}}\right).$$

Although the MSE is the same regardless of \mathbf{T} , the choice of \mathbf{T} affects how the same amount of noise is distributed among the subchannels. We look at two important cases of \mathbf{T} and the respective BER analysis.

- *OFDM System:* The unitary precoder \mathbf{T} is $\mathbf{T} = \mathbf{I}$. We have

$$\sigma_{\text{ofdm}}^2(i) = \mathcal{N}_0/|P_i|^2, \quad i = 0, 1, \dots, M-1. \quad (4)$$

For the i th subchannel, the SNR $\beta_{\text{ofdm}}(i)$ is

$$\beta_{\text{ofdm}}(i) = \gamma|P_i|^2 \quad (5)$$

where γ is the SNR $\mathcal{E}_s/\mathcal{N}_0$. The BER of the OFDM system becomes

$$\mathcal{P}_{\text{ofdm}} = \frac{1}{M} \sum_{i=0}^{M-1} Q\left(\sqrt{\gamma|P_i|^2}\right). \quad (6)$$

- *SC-CP System:* When the unitary precoder \mathbf{T} is the DFT matrix \mathbf{W} , the transmitting matrix $\mathbf{G} = \mathbf{I}$. The unitary matrix \mathbf{T}^\dagger appended to the receiver is \mathbf{W}^\dagger . The resulting system shown in Fig. 4 becomes the SC-CP system [9]. The SC-CP system can be viewed as a precoded OFDM system with precoder $\mathbf{T} = \mathbf{W}$. All the elements in the DFT matrix have the same magnitude, which is equal to $1/\sqrt{M}$. Using this fact and (1), we see that the noise variances in all the subchannels are the same, and they are

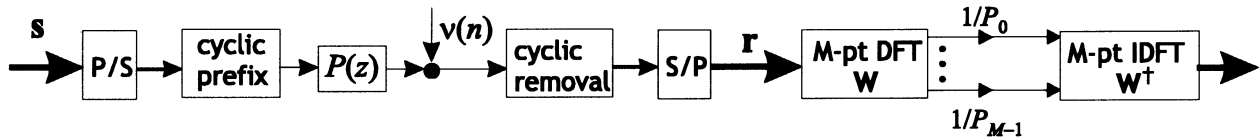


Fig. 4. Block diagram of the SC-CP system over a channel $P(z)$ with additive noise $\nu(n)$.

equal to the average MSE $\sigma_{sc-cp}^2 = \mathcal{E}_{rr}$. As a result, all the subchannels have the same SNR $\beta_{sc-cp} = \mathcal{E}_s/\mathcal{E}_{rr}$ or

$$\beta_{sc-cp} = \frac{1}{\frac{1}{M} \sum_{i=0}^{M-1} \frac{1}{\gamma |P_i|^2}}.$$

The BER of the SC-CP system can be written as

$$\mathcal{P}_{sc-cp} = Q\left(\sqrt{\beta_{sc-cp}}\right). \quad (7)$$

The BER performance of the precoded system is determined by subchannel SNRs. The unitary property of \mathbf{T} allows us to establish upper and lower bounds on the subchannel SNRs.

Lemma 1: For any unitary precoder \mathbf{T} , the i th subchannel SNR $\beta(i)$ is bounded by

$$\min_k \beta_{\text{ofdm}}(k) \leq \beta(i) \leq \max_k \beta_{\text{ofdm}}(k) \quad \text{for } i = 0, 1, \dots, M-1 \quad (8)$$

where $\beta_{\text{ofdm}}(k) = \gamma |P_k|^2$ is the k th subchannel SNR of the OFDM system.

Proof: Using (1) and (4), we observe that the variance of the i th subchannel $\sigma^2(i)$ is given by

$$\sigma^2(i) = \sum_{m=0}^{M-1} |t_{m,i}|^2 \sigma_{\text{ofdm}}^2(m).$$

In addition, by using the fact that \mathbf{T} is unitary with $\mathbf{T}^\dagger \mathbf{T} = \mathbf{I}$, the columns of \mathbf{T} have unit energy, i.e., $\sum_{m=0}^{M-1} |t_{m,i}|^2 = 1$, for all i . We have

$$\sigma^2(i) \leq \sum_{m=0}^{M-1} |t_{m,i}|^2 \max_k \sigma_{\text{ofdm}}^2(k) = \max_k \sigma_{\text{ofdm}}^2(k).$$

Similarly, we can show that $\sigma^2(i) \geq \sum_{m=0}^{M-1} |t_{m,i}|^2 \min_k \sigma_{\text{ofdm}}^2(k) = \min_k \sigma_{\text{ofdm}}^2(k)$. The bounds of SNR $\beta(i)$ follow directly from the bounds of $\sigma^2(i)$. $\triangle\triangle\triangle$

These relations hold for any unitary precoder \mathbf{T} . For a different choice of \mathbf{T} , the noise variances are distributed differently, but they are always bounded between $\min_k \sigma_{\text{ofdm}}^2(k)$ and $\max_k \sigma_{\text{ofdm}}^2(k)$. For any precoder \mathbf{T} , the best subchannel is no better than the best subchannel of the OFDM system, and the worst subchannel is no worse than the worst subchannel of the OFDM system. In the next section, we derive the optimal \mathbf{T} such that the average BER is minimized.

III. OPTIMAL PRECODERS

For the convenience of the following discussion, we introduce the function

$$f(y) \triangleq Q(1/\sqrt{y}). \quad (9)$$

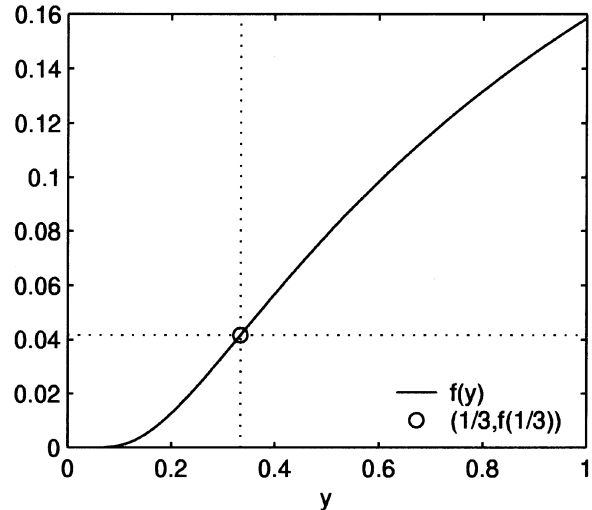


Fig. 5. Plot of $f(y) = Q(1/\sqrt{y})$ for $0 \leq y \leq 1$.

The subchannel BER can be expressed as $\mathcal{P}_T(i) = Q\left(\sqrt{\mathcal{E}_s/\sigma^2(i)}\right) = f(1/\beta(i))$. The BER performance is closely related to the behavior of the function $f(\cdot)$. Important properties of $f(\cdot)$ are given in the following lemma. A proof is given in Appendix A.

Lemma 2: The function $f(y) = Q(1/\sqrt{y})$ is monotone increasing. It is convex when $y \leq 1/3$ and concave when $y > 1/3$.

A plot of $f(y)$ is shown in Fig. 5. Each subchannel is operating in the convex or the concave region of the function $f(\cdot)$, depending on subchannel SNR $\beta(i)$. In particular, when $\beta(i) \geq 3$, the i th subchannel is operating in the convex region of $f(\cdot)$ and $\mathcal{P}_T(i) \leq Q(\sqrt{3}) = 0.0416$. If $\beta(i) < 3$, the i th subchannel is operating in the concave region, and $\mathcal{P}_T(i) > 0.0416$. We define three useful SNR quantities

$$\gamma_0 = \min_i \frac{3}{|P_i|^2}, \quad \bar{\gamma} = \frac{1}{M} \sum_{i=0}^{M-1} \frac{3}{|P_i|^2}, \quad \gamma_1 = \max_i \frac{3}{|P_i|^2}.$$

By definition, they satisfy $\gamma_0 \leq \bar{\gamma} \leq \gamma_1$. We also define three SNR regions:

$$\mathcal{R}_{\text{low}} = \{\gamma | \gamma \leq \gamma_0\}, \quad \mathcal{R}_{\text{mid}} = \{\gamma | \gamma_0 < \gamma < \gamma_1\}$$

$$\mathcal{R}_{\text{high}} = \{\gamma | \gamma_1 \geq \gamma\}.$$

When $\gamma = \bar{\gamma}$, we have $\beta_{sc-cp} = 3$, i.e., the subchannels of the SC-CP system operating on the boundary between the convex and the concave regions of $f(\cdot)$. For the two SNR regions \mathcal{R}_{low} and \mathcal{R}_{mid} , the following can be observed.

- For the SNR region \mathcal{R}_{low} , $\gamma \leq \gamma_0$, and all the subchannels in the OFDM system have SNR $\beta_{\text{ofdm}}(i) \leq 3$ for all i . In addition, using Lemma 1, we know that $\beta(i) \leq 3$ for any unitary precoder \mathbf{T} . Therefore, all the subchannels are

operating in the concave region of $f(y)$ for any precoder \mathbf{T} .

- For the SNR region $\mathcal{R}_{\text{high}}$, $\gamma \geq \gamma_1$. In this case, all the subchannels in the OFDM system have SNR $\beta_{\text{ofdm}}(i) \geq 3$. Moreover, the results in Lemma 1 imply that for an arbitrary unitary precoder \mathbf{T} , we always have $\beta(i) \geq 3$; all the subchannels are operating in the convex region of the function $f(y)$ for any precoder \mathbf{T} .

For \mathcal{R}_{low} and $\mathcal{R}_{\text{high}}$, we can establish the following relations among the BER performances of the three systems OFDM, SC-CP, and an OFDM system with an arbitrary unitary precoder \mathbf{T} . A proof is given in Appendix B.

Theorem 1: Let \mathcal{P}_T be the BER of the OFDM system with a unitary precoder \mathbf{T} in Fig. 2. Then

$$\begin{aligned} \mathcal{P}_{\text{ofdm}} &\leq \mathcal{P}_T \leq \mathcal{P}_{\text{sc-cp}}, & \text{for } \gamma \in \mathcal{R}_{\text{low}} \\ \mathcal{P}_{\text{ofdm}} &\geq \mathcal{P}_T \geq \mathcal{P}_{\text{sc-cp}}, & \text{for } \gamma \in \mathcal{R}_{\text{high}}. \end{aligned}$$

Each of the two inequalities relating \mathcal{P}_T and $\mathcal{P}_{\text{sc-cp}}$ becomes an equality if and only if subchannel noise variances $\sigma^2(i)$ are equalized, i.e., $\sigma^2(i) = \mathcal{E}_{rr}$, where \mathcal{E}_{rr} is as given in (3).

Channel - Independent Transmitters Achieving $\mathcal{P}_{\text{sc-cp}}$: Theorem 1 states that we have $\mathcal{P}_T = \mathcal{P}_{\text{sc-cp}}$ if and only if $\sigma^2(i)$ are equalized, i.e., $\mathcal{N}_0 \sum_{k=0}^{M-1} |t_{k,i}|^2 / |P_k|^2 = \mathcal{E}_{rr}$, where \mathcal{E}_{rr} is as given in (3). In particular, to have channel independent solutions of \mathbf{T} , we can choose

$$|t_{m,n}| = \frac{1}{\sqrt{M}}, \quad 0 \leq m, n \leq M-1. \quad (10)$$

In this case, all the subchannel BERs are the same: $\mathcal{P}_T(i) = \mathcal{P}_T = \mathcal{P}_{\text{sc-cp}}$. There are many unitary matrices satisfying (10). Two well-known solutions satisfying (10) are the DFT matrix \mathbf{W} and the Hadamard matrix \mathbf{H} [18]. When $\mathbf{T} = \mathbf{W}$, the transmitting matrix $\mathbf{G} = \mathbf{I}$, and the transceiver in Fig. 2 becomes the SC-CP system in [9]. The Hadamard matrices can be generated recursively for M , that is, a power of 2. The 2×2 Hadamard matrix is given by

$$\mathbf{H}_2 = \frac{1}{\sqrt{2}} \begin{pmatrix} 1 & 1 \\ 1 & -1 \end{pmatrix}.$$

The $2n \times 2n$ Hadamard matrix can be given in terms of the $n \times n$ Hadamard matrix by

$$\mathbf{H}_{2n} = \frac{1}{\sqrt{2}} \begin{pmatrix} \mathbf{H}_n & \mathbf{H}_n \\ \mathbf{H}_n & -\mathbf{H}_n \end{pmatrix}.$$

The Hadamard matrix is real with elements equal to ± 1 . The resulting transmitting matrix $\mathbf{G} = \mathbf{W}^\dagger \mathbf{H}$ will be complex. The implementation of Hadamard matrices requires only additions. The complexity of the transceiver is slightly more than the OFDM system due to the two extra Hadamard matrices.

When we have a unitary \mathbf{T} that has the equal magnitude property in (10), we can use \mathbf{T} to generate other unitary matrices satisfying the equal magnitude property. For example, consider a matrix \mathbf{T}' with

$$t'_{m,n} = e^{j(\theta_m + \alpha_n)} t_{m,n}, \quad 0 \leq m, n \leq M-1$$

for arbitrary real choices of θ_m and α_n . The new matrix \mathbf{T}' is also unitary, and it has the equal magnitude property.

BER of Precoded OFDM Systems in Different SNR Regions: The results in Theorem 1 imply that the conventional OFDM system ($\mathbf{T} = \mathbf{I}$) is the optimal solution for γ in \mathcal{R}_{low} . When all the subchannels are operating in the concave region of $f(\cdot)$, the OFDM system has the smallest error rate. For γ in $\mathcal{R}_{\text{high}}$, it is the worst solution; when all the subchannels are operating in the convex region of $f(\cdot)$, the OFDM system has the largest error rate. However, as we will see next, the SNR region \mathcal{R}_{low} corresponds to a high error rate, whereas $\mathcal{R}_{\text{high}}$ corresponds to a more useful range of BER. The error rate behavior can be analyzed by considering the value of γ in the following three regions.

- 1) The case \mathcal{R}_{low} : In this range, the OFDM system is the optimal solution. All the subchannels have $\beta_{\text{ofdm}}(k) \leq 3$, and hence, $\mathcal{P}_{\text{ofdm}} \geq Q(\sqrt{3}) = 0.0416$. In this range of SNR, the error rate $\mathcal{P}_{\text{ofdm}}$ is at least 0.0416, which is a BER that is too large for many applications. Furthermore, the minimum error rate 0.0416 can be achieved only when all the subchannels have $\mathcal{P}_{\text{ofdm}}(i) = 0.0416$, which is true only in the special case $|P_0| = |P_1| = \dots = |P_{M-1}|$.
- 2) The case $\mathcal{R}_{\text{high}}$: For this range, the OFDM system has the largest BER, and the BERs of all precoded OFDM systems are lower bounded by $\mathcal{P}_{\text{sc-cp}}$. All subchannels are operating in the convex region of $f(\cdot)$, and $\beta(k) \geq 3$. The subchannel error rate $\mathcal{P}_T(k)$ is less than $Q(\sqrt{3})$, and the average $\mathcal{P}_T \leq 0.0416$. Notice that when $\gamma = \gamma_1$, the worst subchannel of the OFDM system has an error rate $Q(\sqrt{3}) = 0.0416$, and the average BER is at least $Q(\sqrt{3})/M$. Therefore, γ_1 is also the minimum SNR to have an error rate lower than $Q(\sqrt{3})/M$ in the OFDM system. For example, for $M = 16$, γ_1 is the smallest SNR for the OFDM system, to achieve an error rate $Q(\sqrt{3})/16 = 0.0026$. For $M = 64$, γ_1 is the smallest SNR for achieving a BER $Q(\sqrt{3})/64 = 6.4 \times 10^{-4}$. The SNR region $\mathcal{R}_{\text{high}}$ corresponds to a more useful range of BER.
- 3) The case \mathcal{R}_{mid} : We can plot $\mathcal{P}_{\text{sc-cp}}$ and $\mathcal{P}_{\text{ofdm}}$ as functions of γ . The curves of $\mathcal{P}_{\text{ofdm}}$ and $\mathcal{P}_{\text{sc-cp}}$ cross in this range as $\mathcal{P}_{\text{ofdm}}$ is smaller than $\mathcal{P}_{\text{sc-cp}}$ for $\gamma \leq \gamma_0$ and larger than $\mathcal{P}_{\text{sc-cp}}$ for $\gamma \geq \gamma_1$. In most of our experiments, the crossing of the two curves happens at an SNR close to $\bar{\gamma}$, i.e., the SNR for which the subchannels of the SC-CP system fall in the convex region of the function $f(\cdot)$.

Remarks: When the channel has a spectral null, say $P_{i_0} = 0$, the subchannel noise variances in the SC-CP system given in (3) go to infinity. The average probability of error is half in all subchannels, regardless of the value of SNR. In this case, γ_1 goes to infinity, and the SC-CP system is not an optimal solution for any SNR. Such cases can be avoided by using an MMSE receiver, to be discussed in Section V.

IV. OTHER MODULATION SCHEMES

The derivations in Sections II and III are carried out for QPSK modulation. Using approximations of BER obtained from symbol error rate (SER), we can extend the results to

PAM, QAM, and PSK with slight modifications. Optimal precoders are obtained based on BER approximation formulae. We will take QAM modulation as an example. Suppose the inputs are N -ary QAM symbols with variance \mathcal{E}_s . The subchannel SER can be approximated by [19]

$$\mathcal{P}_{T, \text{SER}}(i) \approx 4 \left(1 - \frac{1}{\sqrt{N}}\right) Q \left(\sqrt{\frac{3}{(N-1)} \beta(i)} \right) \quad (11)$$

where $\beta(i) = \mathcal{E}_s/\sigma^2(i)$ is the SNR in the i th subchannel. When Gray code is used, BER $\mathcal{P}_T(i)$ can be approximated from SER as $\mathcal{P}_T(i) \approx \mathcal{P}_{T, \text{SER}}(i)/\log_2 N$ [19]. Therefore, we have

$$\begin{aligned} \mathcal{P}_T &= \frac{1}{M} \sum_{i=0}^{M-1} \mathcal{P}_T(i) \\ &\text{where } \mathcal{P}_T(i) \approx \alpha Q \left(\sqrt{c\beta(i)} \right) \\ &\alpha = \frac{4}{\log_2 N} \left(1 - \frac{1}{\sqrt{N}}\right) \\ &\text{and } c = 3/(N-1). \end{aligned} \quad (12)$$

The subchannel SNRs observe the same bounds given in (8), $\min_k \beta_{\text{ofdm}}(k) \leq \beta(i) \leq \max_k \beta_{\text{ofdm}}(k)$. When SNR γ is large enough such that all the subchannels satisfy $c\beta_{\text{ofdm}}(i) \geq 3$, equalizing the subchannel noise variances will minimize the approximated BER given in (12). The condition for this is

$$\gamma \geq \gamma_1, \quad \text{where } \gamma_1 = \max_k \frac{(N-1)}{|P_k|^2}. \quad (13)$$

On the other hand, when $c\beta_{\text{ofdm}}(i) \leq 3$ for all i , the conventional OFDM system is the optimal transceiver. The condition for this is $\gamma \leq \gamma_0$, where γ_0 is now $\min_k ((N-1)/|P_k|^2)$. The conditions now depend on the QAM constellation. For a large constellation, i.e., larger N , both γ_0 and γ_1 also become larger.

Similarly, the above technique is valid for any modulation scheme in which the subchannel symbol error probability can be either approximated or expressed as

$$\alpha Q \left(\sqrt{c\beta(k)} \right) = \alpha f \left(\frac{1}{c\beta(k)} \right)$$

for some constants α and c that are independent of subchannels. Examples of such a case include PAM, QAM, and PSK modulation schemes. Once the error probability is in such a form, we can invoke the convexity and concavity of $f(\cdot)$ to obtain the SNR ranges for which the OFDM system or the SC-CP system is optimal.

Remark: For real modulation symbols, e.g., PAM, the noise relevant for symbol detection of the i th subchannel is only the real part of e_i but not the imaginary part. The subchannel noise e_i has equal variance in real and imaginary parts. Therefore, the relevant noise variance is $E[|e_i|^2]/2$, which should be used in the evaluation of $\beta(i)$, i.e., $\beta(i) = \mathcal{E}_s/(E[|e_i|^2]/2)$.

V. MMSE TRANSCEIVERS

In this section, we consider the case that the receiver is one that has MMSE. We will show how to derive the optimal

precoder for an MMSE receiver. We will see that using an MMSE receiver improves the system performance, especially when the channel has spectral nulls. The following lemma gives the MMSE receiving matrix \mathbf{S} for a given unitary precoder (the proof is given in Appendix C).

Lemma 3: Consider the precoded OFDM transceiver in Fig. 2. Suppose the inputs have zero mean and variance \mathcal{E}_s , with real and imaginary parts having equal variances $\mathcal{E}_s/2$. The noise is circular complex Gaussian with variance \mathcal{N}_0 . Let \mathbf{x} be the receiver output, and let the error vector $\mathbf{e} = \mathbf{x} - \mathbf{s}$. For a given unitary transmitting matrix $\mathbf{G} = \mathbf{W}^\dagger \mathbf{T}$, the optimal receiving matrix \mathbf{S} that minimizes $E[\mathbf{e}^\dagger \mathbf{e}]$ is given by

$$\begin{aligned} \mathbf{S} &= \mathbf{T}^\dagger \mathbf{\Lambda} \mathbf{W}, \quad \text{where } \mathbf{\Lambda} = \text{diag}(\lambda_0 \ \lambda_1 \ \dots \ \lambda_{M-1}) \\ \lambda_k &= \frac{\gamma P_k^*}{1 + \gamma |P_k|^2}, \quad \gamma = \frac{\mathcal{E}_s}{\mathcal{N}_0}. \end{aligned} \quad (14)$$

The real and imaginary parts of e_i have equal variance. The average MSE $\mathcal{E}_{rr} = E[\mathbf{e}^\dagger \mathbf{e}]$ is $\mathcal{E}_{rr} = (1/M) \sum_{i=0}^{M-1} (\mathcal{E}_s/(1 + \gamma |P_i|^2))$. In this case, the i th receiver output x_i can be expressed as

$$\begin{aligned} x_i &= a_i s_i + \tau_i \\ &\text{where } a_i = \sum_{k=0}^{M-1} |t_{k,i}|^2 \frac{\gamma |P_k|^2}{1 + \gamma |P_k|^2} \\ \tau_i &= \sum_{j \neq i} s_j \sum_{k=0}^{M-1} t_{k,i}^* t_{k,j} \frac{\gamma |P_k|^2}{1 + \gamma |P_k|^2} \\ &\quad + [\mathbf{T}^\dagger \mathbf{\Lambda} \mathbf{W} \mathbf{v}]_i. \end{aligned} \quad (15)$$

For the i th subchannel, the variance of interference plus noise is $E[|\tau_i|^2]$. The subchannel signal-to-interference-noise-ratio (SINR) $\beta(i) = a_i^2 \mathcal{E}_s / E[|\tau_i|^2]$ is given by

$$\beta(i) = \left(\sum_{k=0}^{M-1} \frac{|t_{k,i}|^2 \gamma |P_k|^2}{1 + \gamma |P_k|^2} \right) / \left(\sum_{k=0}^{M-1} \frac{|t_{k,i}|^2}{1 + \gamma |P_k|^2} \right) \quad i = 0, 1, \dots, M-1. \quad (16)$$

From the above lemma, we see that the average MSE \mathcal{E}_{rr} is also independent of the choice of \mathbf{T} like the zero forcing case. The MMSE receiver can be easily obtained from the zero forcing receiver by replacing the M channel-dependent scalars from $1/P_i$ to λ_i given in (14).

When an MMSE receiver is used, the system is not ISI free, and the error does not come from channel noise alone. The term τ_i is a mixture of channel noise and signals from all the other subchannels. However, Gaussian tail renders a very nice approximation of BER [20]–[22], as we will see later in examples. The approximation is extremely good for a reasonably large M , e.g., $M \geq 32$. Throughout the rest of the paper, we will use the Gaussian assumption.

The computation of BER depends on the modulation scheme used. We will use QPSK as an example. The results in Lemma 3 tell us that subchannel errors have equal variances in real and imaginary parts; therefore, the real and imaginary parts of the QPSK symbols have equal probability of error. The BER of the

i th subchannel is $Q(\sqrt{\beta(i)})$. To simplify derivations, let us define

$$h(y) \triangleq Q\left(\sqrt{y^{-1}-1}\right).$$

Then, the subchannel BER is

$$Q\left(\sqrt{\beta(i)}\right) = h\left(\frac{1}{1+\beta(i)}\right).$$

Using (16), we can verify that the argument of $h(\cdot)$ in the above equation can be expressed as

$$\frac{1}{1+\beta(i)} = \sum_{k=0}^{M-1} \frac{|t_{k,i}|^2}{1+\gamma|P_k|^2}. \quad (17)$$

Therefore, we have

$$\mathcal{P}_{T, \text{MMSE}} = \frac{1}{M} \sum_{i=0}^{M-1} \mathcal{P}_{T, \text{MMSE}}(i)$$

$$\text{where } \mathcal{P}_{T, \text{MMSE}}(i) = h\left(\sum_{k=0}^{M-1} \frac{|t_{k,i}|^2}{1+\gamma|P_k|^2}\right). \quad (18)$$

For the conventional OFDM system, the precoder \mathbf{T} is the identity matrix. We can see from (16) that the subchannel SINR is $\gamma|P_i|^2$: the same as that in the zero-forcing case (5); an OFDM system with a zero-forcing receiver has the same performance as that with an MMSE receiver. For the SC-CP system, \mathbf{T} is the DFT matrix with $|t_{k,i}| = 1/\sqrt{M}$. Using the definition of $h(\cdot)$, the BERs of OFDM and SC-CP systems are given, respectively, by

$$\begin{aligned} \mathcal{P}_{\text{ofdm}, \text{mmse}} &= \mathcal{P}_{\text{ofdm}} = \frac{1}{M} \sum_{i=0}^{M-1} h\left(\frac{1}{1+\gamma|P_i|^2}\right) \\ \mathcal{P}_{\text{sc-cp}, \text{mmse}} &= h\left(\frac{1}{M} \sum_{i=0}^{M-1} \frac{1}{1+\gamma|P_i|^2}\right). \end{aligned} \quad (19)$$

Lemma 4: The function $h(y) = Q(\sqrt{y^{-1}-1})$ defined for $0 < y < 1$ is convex with $h'(y) > 0$ and $h''(y) \geq 0$.

The lemma is proved in Appendix D. A plot of $h(y)$ for $0 < y < 1$ is given in Fig. 6. We only need to consider that the interval $0 < y < 1$ as the argument of $h(\cdot)$ in (18) is in this range. Using the convexity of $h(\cdot)$, we can show the following theorem.

Theorem 2: Let $\mathcal{P}_{T, \text{MMSE}}$, as given in (18), be the BER of the MMSE-equalized precoded OFDM systems with a unitary precoder \mathbf{T} . Then

$$\mathcal{P}_{\text{sc-cp}, \text{mmse}} \leq \mathcal{P}_{T, \text{MMSE}} \leq \mathcal{P}_{\text{ofdm}}.$$

The first inequality becomes an equality if and only if subchannel SINRs $\beta(i)$ are equalized.

Proof: Using (17) and the fact that the SINR $\beta_{\text{ofdm}}(k) = \gamma|P_k|^2$, we can see that

$$\min_k \frac{1}{1+\gamma|P_k|^2} \leq \frac{1}{1+\beta(i)} \leq \max_k \frac{1}{1+\gamma|P_k|^2}$$

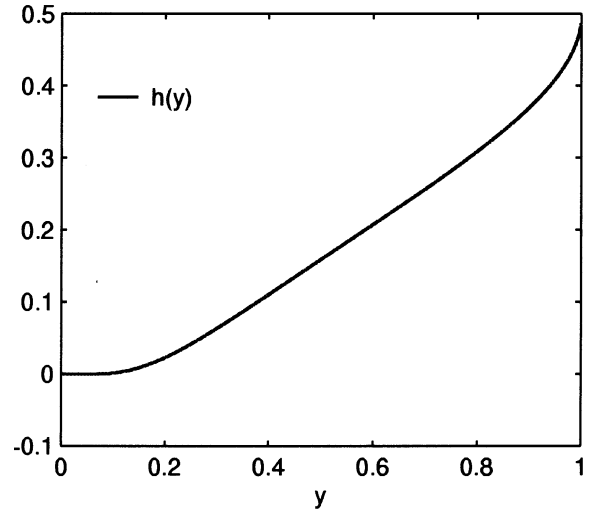


Fig. 6. Plot of $h(y) = Q(\sqrt{y^{-1}-1})$ for $0 \leq y \leq 1$.

for $i = 0, 1, \dots, M-1$.

As in the proof in Theorem 1, we can use the convexity of $h(\cdot)$ to show that

$$\begin{aligned} h\left(\frac{1}{M} \sum_{k=0}^{M-1} \frac{1}{1+\gamma|P_k|^2}\right) &\leq \mathcal{P}_{T, \text{MMSE}} = \frac{1}{M} \sum_{i=0}^{M-1} h\left(\frac{1}{1+\gamma|P_i|^2}\right) \\ &\leq \frac{1}{M} \sum_{k=0}^{M-1} h\left(\frac{1}{1+\gamma|P_k|^2}\right). \end{aligned}$$

The lower and upper bounds are, respectively, $\mathcal{P}_{\text{sc-cp}, \text{mmse}}$ and $\mathcal{P}_{\text{ofdm}}$, which are given in (19). $\triangle\triangle\triangle$

As we mentioned in the previous section for the zero forcing receiver, the output noise becomes infinitely large in the presence of spectral null. In the MMSE case, the expression of subchannel SINR $\beta(i)$ in (16) indicates that even if the channel has spectral nulls, $\beta(i)$ is not zero.

Optimal Precoders: Theorem 2 states that the minimum $\mathcal{P}_{\text{sc-cp}, \text{mmse}}$ is achieved, if and only if $\beta(i)$ are equalized. Observing (16), we see that $\beta(i)$ can be equalized by choosing \mathbf{T} , which has the equal magnitude property in (10). The same class of \mathbf{T} achieving $\mathcal{P}_{\text{sc-cp}}$ in the zero forcing case is also optimal for the MMSE case. Again, the Hadamard matrix along with the DFT matrix are examples of such solutions. On the other hand, the conventional OFDM system, although optimal for low SNR in zero-forcing case, is the worst solution in MMSE case for all SNR γ .

Other Modulation Schemes: For modulations other than QPSK, we can use approximations of BER from SER as in Section IV. The results will be stated without proofs. We will use N -ary QAM as an example. By (11), $\mathcal{P}_{T, \text{MMSE}}(i) \approx \alpha Q(\sqrt{c\beta(i)})$, where $\beta(i)$ is as given in (16). Let us define

$$g(y) = \alpha Q(\sqrt{c(y^{-1}-1)}).$$

Then

$$\mathcal{P}_{T, \text{MMSE}}(i) \approx \alpha Q(\sqrt{c\beta(i)}) = g\left(\frac{1}{1+\beta(i)}\right).$$

Similar to the QPSK case, we can use (16) to express the argument of $g(\cdot)$ in the above equation as $1/(1 + \beta(i)) = \sum_{k=0}^{M-1} (|t_{k,i}|^2 / (1 + \gamma|P_k|^2))$. Therefore, we have

$$\mathcal{P}_{T, \text{MMSE}} = \frac{1}{M} \sum_{i=0}^{M-1} \mathcal{P}_{T, \text{MMSE}}(i)$$

$$\text{where } \mathcal{P}_{T, \text{MMSE}}(i) = g\left(\sum_{k=0}^{M-1} \frac{|t_{k,i}|^2}{1 + \gamma|P_k|^2}\right). \quad (20)$$

To exploit the convexity and the concavity of $g(\cdot)$, we define

$$\mathcal{R}_0 = [0, z_0], \quad \mathcal{R}_1 = (z_0, z_1), \quad \text{and} \quad \mathcal{R}_2 = [z_1, 1]$$

$$\text{where } z_0 = \frac{3c + 1 - \sqrt{9c^2 - 10c + 1}}{8c}$$

$$\text{and } z_1 = \frac{3c + 1 + \sqrt{9c^2 - 10c + 1}}{8c}.$$

We can show that $g(y)$ is convex over \mathcal{R}_0 and \mathcal{R}_2 , and it is concave over \mathcal{R}_1 . Notice that when $1/(1 + \beta(i)) \leq z_0$, the i th subchannel is operating in the convex region \mathcal{R}_0 of $g(\cdot)$. For the conventional OFDM system, the condition for this is

$$\gamma \geq \frac{z_0^{-1} - 1}{|P_i|^2}. \quad (21)$$

Similarly, when γ and P_i are such that

$$\gamma \leq \frac{z_1^{-1} - 1}{|P_i|^2} \quad (22)$$

the i th subchannel of the conventional OFDM system is operating in the convex region \mathcal{R}_2 . When SNR is high enough so that (21) is true for all i or when the SNR is low enough so that (22) is true for all i , all the subchannels of the conventional OFDM system will operate in one of the convex regions of $g(\cdot)$. In this case, we can invoke the convexity of $g(\cdot)$ to show that the class of unitary matrices satisfying the equal magnitude property in (10) are optimal. It can be verified that the case \mathcal{R}_2 corresponds to a very high error rate, whereas \mathcal{R}_0 corresponds to a more useful range. To have all subchannels operating in \mathcal{R}_0 , we need

$$\gamma \geq \gamma'_1, \quad \text{where } \gamma'_1 = \max_i \frac{z_0^{-1} - 1}{|P_i|^2}.$$

It can be further verified that γ'_1 is less than the value of γ_1 given in (13). This means that $\mathcal{P}_{\text{sc-cp, mmse}}$ becomes the minimum BER at a smaller SNR than $\mathcal{P}_{\text{sc-cp}}$.

VI. SIMULATION EXAMPLES

We will assume that the noise is AWGN with variance \mathcal{N}_0 . The modulation symbols are QPSK with values equal to $\pm\sqrt{\mathcal{E}_s/2} \pm j\sqrt{\mathcal{E}_s/2}$ and SNR $\gamma = \mathcal{E}_s/\mathcal{N}_0$. The number of subchannels M is 64. The length of cyclic prefix is 3. Two channels with four coefficients ($L = 3$) will be used in the first three examples: $p_1(n)$: 0.3903 + j 0.1049, 0.6050 + j 0.1422, 0.4402 + j 0.0368, 0.0714 + j 0.5002, and $p_2(n)$: -0.3699 - j 0.5782, -0.4053 - j 0.5750, -0.0834 - j 0.0406, 0.1587 - j 0.0156. The magnitude responses of the two channels $p_1(n)$ and $p_2(n)$ are shown in

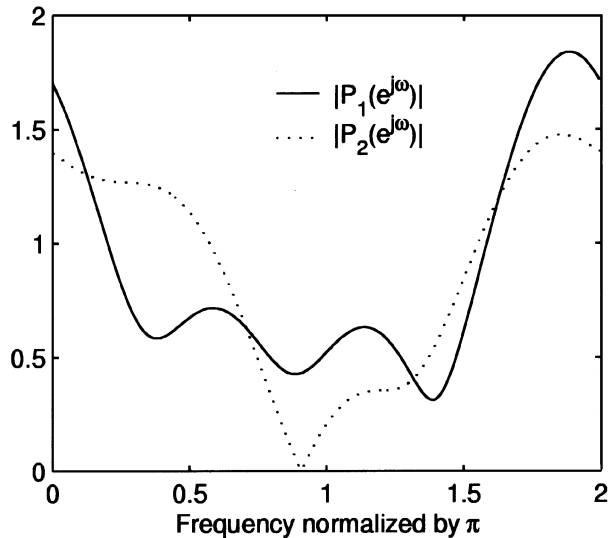


Fig. 7. Frequency responses of the two channels $p_1(n)$ and $p_2(n)$.

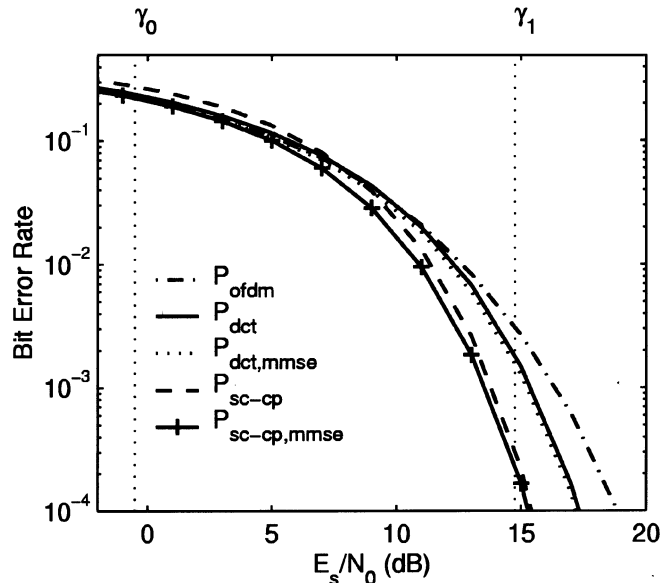


Fig. 8. Example 1. Performance comparison of $\mathcal{P}_{\text{ofdm}}$, \mathcal{P}_{dct} , $\mathcal{P}_{\text{dct, mmse}}$, $\mathcal{P}_{\text{sc-cp}}$, and $\mathcal{P}_{\text{sc-cp, mmse}}$ for the channel $p_1(n)$.

Fig. 7. The BER performance is obtained through Monte Carlo simulation, unless otherwise mentioned.

Example 1: We will use $p_1(n)$ in this example. We compute the values of $\gamma_0 = \min_i 3/|P_i|^2$, $\bar{\gamma} = 1/M \sum_{i=0}^{M-1} 3/|P_i|^2$, and $\gamma_1 = \max_i 3/|P_i|^2$, respectively, as -0.51, 8.85, and 14.74 dB.

Fig. 8 shows $\mathcal{P}_{\text{ofdm}}$ and $\mathcal{P}_{\text{sc-cp}}$ as functions of SNR γ . We also show the BER for the case when the transmitting matrix \mathbf{G} is a unitary type II DCT matrix, which is denoted as \mathcal{P}_{dct} . In this case, the precoder \mathbf{T} given by $\mathbf{W}\mathbf{G}$ does not have the unit magnitude property in (10). Whenever SNR $\gamma = \mathcal{E}_s/\mathcal{N}_0$ is larger than $\gamma_1 = 14.74$ dB, $\mathcal{P}_{\text{sc-cp}}$ given in (7) becomes the minimum BER for any unitary precoder \mathbf{T} . For $\gamma \leq \gamma_0$, the conventional OFDM system is the optimal solution. For $\gamma = \gamma_0$, we observe that $\mathcal{P}_{\text{ofdm}} \approx 0.2$. In this case, the OFDM system is optimal only for BER larger than 0.2. For either SNR range, $\gamma \leq \gamma_0$ or $\gamma \geq \gamma_1$, and the performance of \mathcal{P}_{dct} is in between

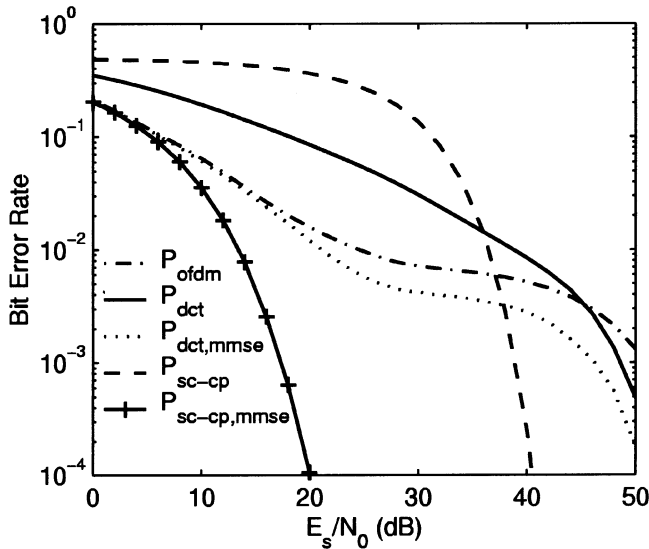


Fig. 9. Example 2. Performance comparison of $\mathcal{P}_{\text{ofdm}}$, \mathcal{P}_{dct} , $\mathcal{P}_{\text{dct,mmse}}$, $\mathcal{P}_{\text{sc-cp}}$, and $\mathcal{P}_{\text{sc-cp,mmse}}$ for the channel $p_2(n)$.

$\mathcal{P}_{\text{ofdm}}$ and $\mathcal{P}_{\text{sc-cp}}$. The BER performances of MMSE receivers $\mathcal{P}_{\text{dct,mmse}}$ and $\mathcal{P}_{\text{sc-cp,mmse}}$ are also shown in the same plot. In each case, the BER of the MMSE receiver is lower than the zero-forcing receiver for all SNR. For the OFDM system, an MMSE receiver does not improve BER: $\mathcal{P}_{\text{ofdm}} = \mathcal{P}_{\text{ofdm,mmse}}$. In addition, observe that the crossing of $\mathcal{P}_{\text{sc-cp}}$ and $\mathcal{P}_{\text{ofdm}}$ occurs around BER = 0.04 and $\gamma = 8$ dB, which is a value very close to $\bar{\gamma} = 8.85$ dB.

Example 2: The channel in this example $p_2(n)$ has a spectral null around 0.9π (see Fig. 7). The DFT coefficients around 0.9π are very small. The values of γ_0 , $\bar{\gamma}$, and γ_1 are, respectively, 1.4, 33.8, and 51.9 dB. Fig. 9 shows the five BER performance curves as in the previous example, $\mathcal{P}_{\text{ofdm}}$, \mathcal{P}_{dct} , $\mathcal{P}_{\text{dct,mmse}}$, $\mathcal{P}_{\text{sc-cp}}$, and $\mathcal{P}_{\text{sc-cp,mmse}}$. Due to the zero close to the unit circle, the BERs of the three zero forcing systems $\mathcal{P}_{\text{ofdm}}$, \mathcal{P}_{dct} , and $\mathcal{P}_{\text{sc-cp}}$ become small only for large SNR. However, there is no serious performance degradation in the SC-CP system with an MMSE receiver. Notice that the crossing of $\mathcal{P}_{\text{sc-cp}}$ and $\mathcal{P}_{\text{ofdm}}$ occurs around $\gamma = 37$ dB, which is a value closer to $\bar{\gamma} = 33.8$ dB than to $\gamma_0 = 1.4$ dB or $\gamma_1 = 51.9$ dB. The BER corresponding to the crossing is 6×10^{-3} .

Example 3: In this example, the channel is $p_1(n)$, like in Example 1. We plot the actual BER and the approximation $\mathcal{P}_{T, \text{MMSE}}$ computed from (18) (see Fig. 10). For the SNR grid considered in the plot, the actual BER is obtained by Monte Carlo simulation. Two cases are shown: the SC-CP system and the case that the transmitting matrix \mathbf{G} is a DCT matrix. We can see that in both cases, the approximations are indistinguishable from the actual BER. This example demonstrates that even though output errors consist of ISI terms and channel noise, the BER is well approximated by Gaussian tail for all SNR. We will use (18) in the next example to compute BER over a fading channel.

Example 4: We use a multipath fading channel with four coefficients. The coefficients are obtained from independent circular complex Gaussian random variables with zero mean and variances given, respectively, by 8/15, 4/15, 2/15, and

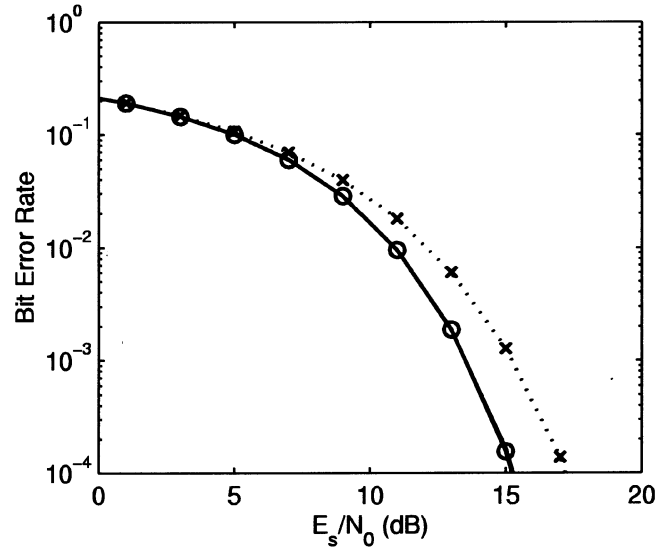


Fig. 10. Example 3. Comparison of the actual BER and the BER $\mathcal{P}_{T, \text{MMSE}}$ computed from (18). For the DCT case, the actual BER is the dotted line, and $\mathcal{P}_{\text{dct,mmse}}$ is the dotted line marked with "x." For the SC-CP system, the actual BER is the solid line, and $\mathcal{P}_{\text{sc-cp,mmse}}$ is the solid line marked with "o."

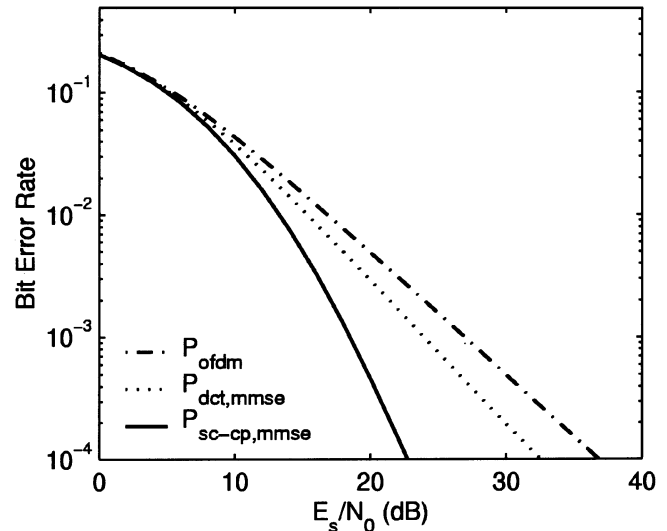


Fig. 11. Example 4. BER performances $\mathcal{P}_{\text{ofdm}}$, $\mathcal{P}_{\text{dct,mmse}}$, and $\mathcal{P}_{\text{sc-cp,mmse}}$ over a four-tap fading channel.

1/15. We compute the BER performances $\mathcal{P}_{\text{ofdm}}$, $\mathcal{P}_{\text{dct,mmse}}$, and $\mathcal{P}_{\text{sc-cp,mmse}}$ using (18) and average the results for 20 000 random channels (see Fig. 11). For high SNR range, $\mathcal{P}_{\text{sc-cp,mmse}}$ requires a significantly smaller transmission power than $\mathcal{P}_{\text{ofdm}}$ for the same BER. The performance of $\mathcal{P}_{\text{dct,mmse}}$ is in between $\mathcal{P}_{\text{sc-cp,mmse}}$ and $\mathcal{P}_{\text{ofdm}}$ for all SNR.

VII. CONCLUSIONS

In the context of transceiver designs, the optimality addressed in most of the earlier works is in the sense of mean squared error minimization. In the paper, we consider directly the minimization of uncoded BER for the class of OFDM transceivers with unitary precoders. For QPSK signaling and MMSE reception, there exist channel-dependent optimal precoders. This is

the class of unitary matrices \mathbf{T} with the equal magnitude property, i.e., $|t_{m,n}| = 1/\sqrt{M}$, for $0 \leq m, n \leq M-1$. One of the solutions is the DFT matrix, and the resulting transceiver is the SC-CP system. In the case of zero-forcing receivers, the solution of optimal precoders depends on SNR. For higher SNR associated with a practical range of BER, the optimal precoders that are channel independent are also the set of unitary matrices with the equal magnitude property. In the presence of channel spectral nulls, the performance of zero-forcing receivers exhibits serious degradation. Robustness against channel spectral nulls can be achieved by using MMSE receivers.

APPENDIX A PROOF OF LEMMA 2

Let $u(y) \triangleq 1/\sqrt{y}$ for $y \geq 0$; then, $f(y) = Q(u(y))$. The lemma can be proved by computing the first and second derivative of $f(y)$. The function $u(y) \triangleq 1/\sqrt{y}$ for $y \geq 0$ is convex with first derivative $u'(y) = -(1/2)y^{-3/2}$ and second derivative $u''(y) = (3/4)y^{-5/2}$. The function $Q(x)$ for $x \geq 0$ is also convex with $Q'(x) = -(1/\sqrt{2\pi})e^{-x^2/2}$ and

$$Q''(x) = \frac{x}{\sqrt{2\pi}} e^{-x^2/2}.$$

The first derivative $f'(y) = Q'(u(y))u'(y)$ is given by $f'(y) = (1/2\sqrt{2\pi})e^{-(1/2y)}y^{-3/2}$, which means that $f(y)$ is strictly monotone increasing. We can verify that $f''(y) = Q''(u(y))[u'(y)]^2 + Q'(u(y))u''(y)$ can be expressed as

$$f''(y) = \frac{1}{4\sqrt{2\pi}} e^{-(1/2y)}y^{-7/2}(1-3y).$$

Therefore, $f''(y) \geq 0$ for $y \leq 1/3$ and $f''(y) < 0$ for $y > 1/3$, which proves the lemma.

APPENDIX B PROOF OF THEOREM 1

We will use the concavity and convexity of $f(\cdot)$ to prove Theorem 1. Given a set of numbers y_0, y_1, \dots, y_{M-1} with $0 \leq y_i \leq 1/3$, the strictly monotone increasing property and the convexity of $f(y)$ imply

$$\sum_{i=0}^{M-1} \lambda_i f(y_i) \geq f\left(\sum_{i=0}^{M-1} \lambda_i y_i\right)$$

where $\lambda_i \geq 0$, and $\sum_{i=0}^{M-1} \lambda_i = 1$.

Similarly, given y_0, y_1, \dots, y_{M-1} with $y_i \geq 1/3$, the concave property of $f(y)$ for $y \geq 1/3$ implies

$$\sum_{i=0}^{M-1} \lambda_i f(y_i) \leq f\left(\sum_{i=0}^{M-1} \lambda_i y_i\right)$$

where $\lambda_i \geq 0$, and $\sum_{i=0}^{M-1} \lambda_i = 1$.

Let us first consider the case $\gamma \geq \gamma_1$. For this range, the subchannel SNR of the OFDM system $\beta_{\text{ofdm}}(i) \geq 3$. For a general unitary precoder \mathbf{T} , we can use (8) to see that whenever

a subchannel has SNR satisfying $\beta(i) \geq 3$, it is operating in the convex region of $f(y)$. We have

$$\mathcal{P}_T = \frac{1}{M} \sum_{i=0}^{M-1} f\left(\frac{1}{\beta(i)}\right) \geq f\left(\frac{1}{M} \sum_{i=0}^{M-1} \frac{1}{\beta(i)}\right) = \mathcal{P}_{\text{sc-cp}}. \quad (23)$$

On the other hand, using (2), we have

$$f\left(\frac{1}{\beta(i)}\right) = f\left(\sum_{k=0}^{M-1} |t_{k,i}|^2 \frac{1}{\gamma|P_k|^2}\right) \leq \sum_{k=0}^{M-1} |t_{k,i}|^2 f\left(\frac{1}{\gamma|P_k|^2}\right).$$

The inequality follows from the fact that $1/(\gamma|P_k|^2)$ is in the convex region of $f(\cdot)$ for $\gamma \geq \gamma_1$. Therefore

$$\begin{aligned} \mathcal{P}_T &= \frac{1}{M} \sum_{i=0}^{M-1} f\left(\frac{1}{\beta(i)}\right) \\ &= \frac{1}{M} \sum_{i=0}^{M-1} f\left(\sum_{k=0}^{M-1} |t_{k,i}|^2 \frac{1}{\gamma|P_k|^2}\right) \\ &\leq \frac{1}{M} \sum_{k=0}^{M-1} \sum_{i=0}^{M-1} |t_{k,i}|^2 f\left(\frac{1}{\gamma|P_k|^2}\right) \\ &= \frac{1}{M} \sum_{k=0}^{M-1} f\left(\frac{1}{\gamma|P_k|^2}\right) = \mathcal{P}_{\text{ofdm}} \end{aligned} \quad (24)$$

where we have used the fact that for any unitary \mathbf{T} , its rows have unit energy $\sum_{i=0}^{M-1} |t_{k,i}|^2 = 1$ for all k . Combining (23) and (24), we obtain $\mathcal{P}_{\text{ofdm}} \geq \mathcal{P}_T \geq \mathcal{P}_{\text{sc-cp}}$ for $\gamma \geq \gamma_1$. Similarly, when $\gamma \leq \gamma_0$, we can use the concavity of $f(\cdot)$ to show that $\mathcal{P}_{\text{ofdm}} \leq \mathcal{P}_T \leq \mathcal{P}_{\text{sc-cp}}$.

APPENDIX C PROOF OF LEMMA 3

Proof: Without loss of generality, we can consider \mathbf{S} as the interconnection $\mathbf{S} = \mathbf{H}\mathbf{\Theta}\mathbf{W}$, where \mathbf{H} is a general $M \times M$ nonsingular matrix, and $\mathbf{\Theta}$ is a diagonal matrix with k th diagonal element $[\mathbf{\Theta}]_{kk} = 1/P_k$. Let \mathbf{y} be the output vector of the matrix $\mathbf{\Theta}$. If we choose $\mathbf{H} = \mathbf{T}^\dagger$, then \mathbf{S} becomes the zero forcing solution. In the absence of channel noise, we have $\mathbf{y} = \mathbf{T}\mathbf{s}$. Therefore, \mathbf{y} can be expressed as $\mathbf{y} = \mathbf{T}\mathbf{s} + \mathbf{q}$, where $\mathbf{q} = \mathbf{\Theta}\mathbf{W}\mathbf{v}$ is a noise vector from the channel noise alone, and $\mathbf{e} = \mathbf{H}\mathbf{y} - \mathbf{s}$. By the orthogonality principle, \mathbf{e} should be orthogonal to the observation vector \mathbf{y} , i.e., $E[(\mathbf{H}\mathbf{y} - \mathbf{s})\mathbf{y}^\dagger] = \mathbf{0}$. This yields $\mathbf{H}\mathbf{E}[\mathbf{y}\mathbf{y}^\dagger] = E[\mathbf{s}\mathbf{y}^\dagger]$. Solving this equation, we get

$$\mathbf{H} = \mathbf{T}^\dagger \underbrace{\mathcal{E}_s (\mathcal{E}_s \mathbf{I} + \mathcal{N}_0 \mathbf{\Theta}\mathbf{\Theta}^\dagger)^{-1}}_{\mathbf{D}} \quad (25)$$

where \mathbf{D} is a diagonal matrix with the k th diagonal element equal to $\mathcal{E}_s/(\mathcal{E}_s + \mathcal{N}_0/|P_k|^2)$. Therefore, the optimal \mathbf{S} is $\mathbf{T}^\dagger \mathbf{D} \mathbf{\Theta} \mathbf{W}$. Letting $\mathbf{\Lambda} = \mathbf{D} \mathbf{\Theta}$, we obtain the expression of \mathbf{S} given in (14). Using \mathbf{H} as in (25), we can further verify that $\mathbf{x} = \mathbf{H}\mathbf{y}$ can be written as $\mathbf{x} = \mathbf{T}^\dagger \mathbf{D} \mathbf{T} \mathbf{s} + \mathbf{T}^\dagger \mathbf{\Lambda} \mathbf{W} \mathbf{v}$. Hence

$$\mathbf{e} = \mathbf{T}^\dagger (\mathbf{D} - \mathbf{I}) \mathbf{T} \mathbf{s} + \mathbf{T}^\dagger \mathbf{\Lambda} \mathbf{W} \mathbf{v}.$$

The input symbols are assumed to be uncorrelated with real and imaginary parts having the same variance \mathcal{E}_s ; the vector $\mathbf{T}s$ has the same statistics, which are implied by the unitary property of \mathbf{T} . Therefore, we have

$$\begin{aligned} E[|e_i|^2] &= \sum_{k=0}^{M-1} |t_{k,i}|^2 \frac{\mathcal{E}_s}{(1 + \gamma|P_k|^2)^2} + \sum_{k=0}^{M-1} |t_{k,i}|^2 \frac{\mathcal{N}_0\gamma^2|P_k|^2}{(1 + \gamma|P_k|^2)^2} \\ &= \sum_{k=0}^{M-1} |t_{k,i}|^2 \frac{\mathcal{E}_s}{1 + \gamma|P_k|^2}. \end{aligned}$$

Therefore, the MSE $\mathcal{E}_{rr} = 1/M \sum_{i=0}^{M-1} E[|e_i|^2]$ is as given in the lemma. We also observe that the error vector consists of two parts $\mathbf{T}^\dagger(\mathbf{D} - \mathbf{I})\mathbf{T}s$ and $\mathbf{T}^\dagger\mathbf{\Lambda}\mathbf{W}\mathbf{v}$. With the assumption that the input \mathbf{s} have equal variance in real and imaginary parts, we can verify that the vector $\mathbf{T}^\dagger(\mathbf{D} - \mathbf{I})\mathbf{T}s$ also has the property that the real and imaginary parts have the same variance. Similarly, the noise vector \mathbf{v} has the same property, and $\mathbf{T}^\dagger\mathbf{\Lambda}\mathbf{W}\mathbf{v}$ also has the same property. Therefore, we conclude that \mathbf{e} has equal variance in real and imaginary parts.

As $\mathbf{x} = \mathbf{T}^\dagger\mathbf{D}\mathbf{T}s + \mathbf{T}^\dagger\mathbf{\Lambda}\mathbf{W}\mathbf{v}$, the i th element x_i has the expression in (15). The variance of x_i is

$$E[|x_i|^2] = \mathcal{E}_s \sum_{k=0}^{M-1} |t_{k,i}|^2 \frac{\gamma|P_k|^2}{1 + \gamma|P_k|^2}.$$

The above expression means that $E[|x_i|^2] = a_i\mathcal{E}_s$ and that $E[|\tau_i|^2] = E[|x_i|^2] - a_i^2\mathcal{E}_s = a_i\mathcal{E}_s - a_i^2\mathcal{E}_s$. The i th subchannel SINR

$$\beta(i) = \frac{a_i^2\mathcal{E}_s}{E[|\tau_i|^2]} = \frac{a_i^2\mathcal{E}_s}{a_i\mathcal{E}_s - a_i^2\mathcal{E}_s} = \frac{a_i}{1 - a_i}.$$

Using the expression of a_i in (15), we obtain $\beta(i)$, as given in (16).

APPENDIX D PROOF OF LEMMA 4

We will prove the lemma by showing that $h'(x) > 0$ and $h''(x) \geq 0$. The function $h(x)$ can be written as $h(y) = f(\eta(y))$, where $\eta(y) = y/(1 - y)$. The first and second derivatives of $\eta(y)$ are, respectively, $\eta'(y) = 1/(1 - y)^2$ and $\eta''(y) = 2/(1 - y)^3$, which are both larger than zero for $0 < y < 1$. The first and second derivatives of $f(y)$ are computed in Appendix A. As $f'(y) > 0$ and $\eta'(y) > 0$, the first derivative $h'(y) = f'(\eta(y))\eta'(y) > 0$. We can verify that the second derivative $h''(y)$ can be rearranged as

$$h''(y) = \frac{1}{4\sqrt{2\pi}} e^{-(1/2\eta(y))} [\eta(y)]^{-3/2} (1 - y)^{-3} y^{-2} (1 - 2y)^2$$

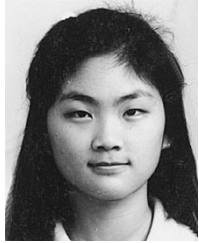
which is larger than or equal to zero.

ACKNOWLEDGMENT

The authors would like to thank the anonymous reviewers for many constructive comments and suggestions that have considerably improved this paper.

REFERENCES

- [1] J. A. C. Bingham, "Multicarrier modulation for data transmission: An idea whose time has come," *IEEE Commun. Mag.*, vol. 26, pp. 5–14, May 1990.
- [2] J. S. Chow, J. C. Tu, and J. M. Cioffi, "A discrete multitone transceiver system for HDSL applications," *IEEE J. Select. Areas Commun.*, vol. 9, pp. 895–908, Aug. 1991.
- [3] A. N. Akansu, P. Duhamel, X. Lin, and M. de Courville, "Orthogonal transmultiplexers in communication: A review," *IEEE Trans. Signal Processing*, vol. 46, pp. 979–995, Apr. 1998.
- [4] L. J. Cimini, "Analysis and simulation of a digital mobile channel using orthogonal frequency division multiple access," *IEEE Trans. Commun.*, vol. 30, pp. 665–675, July 1985.
- [5] I. Kalet, "Multitone modulation," in *Subband and Wavelet Transforms: Design and Applications*, A. N. Akansu and M. J. T. Smith, Eds. Boston, MA: Kluwer, 1995.
- [6] ISO/IEC, "IEEE Std. 802.11a," 1999.
- [7] ETSI, "Digital Audio Broadcasting (DAB) to mobile, portable and fixed receivers," ETS 300 401, 1994.
- [8] ETSI, "Digital Video Broadcasting: Framing, structure, channel coding and modulation for digital terrestrial television (DVB-T)," ETS 300 744, 1997.
- [9] H. Sari, G. Karam, and I. Jeanclaude, *Frequency-Domain Equalization of Mobile Radio and Terrestrial Broadcast Channels*. San Francisco, CA: Glöbecom, 1994.
- [10] D. Falconer, S. L. Ariyavisitakul, A. Benyamin-Seeyar, and B. Eidson, "Frequency domain equalization for single-carrier broadband wireless systems," *IEEE Commun. Mag.*, vol. 40, pp. 58–66, Apr. 2002.
- [11] X. G. Xia, "Precoded and vector OFDM robust to channel spectral nulls and with reduced cyclic prefix length in single transmit antenna systems," *IEEE Trans. Commun.*, vol. 49, pp. 1363–1374, Aug. 2001.
- [12] Z. Wang and G. B. Giannakis, "Linearly precoded or coded OFDM against wireless channel fades?," in *Proc. Third IEEE Workshop Signal Process. Adv. Wireless Commun.*, Taoyuan, Taiwan, R.O.C., Mar. 2001.
- [13] A. Scaglione, G. B. Giannakis, and S. Barbarossa, "Redundant filterbank precoders and equalizers Part I: Unification and optimal designs," *IEEE Trans. Signal Processing*, vol. 47, pp. 1988–2006, July 1999.
- [14] A. Scaglione, S. Barbarossa, and G. B. Giannakis, "Filterbank transceivers optimizing information rate in block transmissions over dispersive channels," *IEEE Trans. Inform. Theory*, vol. 45, pp. 1019–1032, Apr. 1999.
- [15] N. Al-Dhahir and J. Cioffi, "Block transmission over dispersive channels: Transmit filter optimization and realization, and MMSE-DFE receiver performance," *IEEE Trans. Inform. Theory*, vol. 42, pp. 137–160, Jan. 1996.
- [16] Y.-P. Lin and S.-M. Phoong, "Optimal ISI free DMT transceivers for distorted channels with colored noise," *IEEE Trans. Signal Processing*, vol. 49, pp. 2702–2712, Nov. 2001.
- [17] Y. Ding, T. N. Davidson, S.-K. Zhang, Z.-Q. Luo, and K. M. Wong, "Minimum ber block precoders for zero-forcing equalization," in *Proc. IEEE International Conf. Acoust., Speech, Signal Processing*, 2002.
- [18] N. Ahmed and K. R. Rao, *Orthogonal Transforms for Digital Signal Processing*: Springer Verlag, 1975.
- [19] J. G. Proakis, *Digital Communications*. New York: McGraw-Hill, 1995.
- [20] H. V. Poor and S. Verdu, "Probability of error in MMSE multiuser detection," *IEEE Trans. Inform. Theory*, vol. 43, pp. 847–857, May 1997.
- [21] J. Zhang, E. K. P. Chong, and D. N. C. Tse, "Output MAI distribution of linear MMSE multiuser receivers in DS-CDMA system," *IEEE Trans. Inform. Theory*, vol. 47, pp. 1128–1144, Mar. 2001.
- [22] J. Zhang and E. K. P. Chong, "Linear MMSE multiuser receivers: MAI conditional weak convergence and network capacity," *IEEE Trans. Inform. Theory*, vol. 48, pp. 2114–2122, July 2002.
- [23] Y.-P. Lin and S.-M. Phoong, "Analytic BER comparison of OFDM and single carrier systems," in *Proc. Int. Workshop Spectral Methods Multi-rate Signal Process.*, 2002.
- [24] —, "BER optimized channel independent precoder for OFDM system," in *Proc. IEEE Global Telecommun. Conf.*, Taipei, Taiwan, R.O.C., 2002.



Yuan-Pei Lin (S'93–M'97) was born in Taipei, Taiwan, R.O.C., in 1970. She received the B.S. degree in control engineering from the National Chiao-Tung University, Hsinchu, Taiwan, in 1992, and the M.S. and Ph.D. degrees, both in electrical engineering, from the California Institute of Technology, Pasadena, in 1993 and 1997, respectively.

She joined the Department of Electrical and Control Engineering, National Chiao-Tung University, in 1997. Her research interests include digital signal processing, multirate filterbanks, and digital

communication systems with emphasis on multicarrier transmission.

Dr. Lin is currently an associate editor for IEEE TRANSACTIONS ON SIGNAL PROCESSING and an associate editor for the Academic Press journal *Multidimensional Systems and Signal Processing*.



See-May Phoong (M'96) was born in Johor, Malaysia, in 1968. He received the B.S. degree in electrical engineering from the National Taiwan University (NTU), Taipei, Taiwan, R.O.C., in 1991 and the M.S. and Ph.D. degrees in electrical engineering from the California Institute of Technology (Caltech), Pasadena, in 1992 and 1996, respectively.

He was with the Faculty of the Department of Electronic and Electrical Engineering, Nanyang Technological University, Singapore, from September 1996 to September 1997. In September 1997, he joined the

Graduate Institute of Communication Engineering, NTU, as an Assistant Professor, and since August 2001, he has been an Associate Professor. His interests include multirate signal processing and filterbanks and their application to communications.

Dr. Phoong is currently an Associate Editor for the IEEE TRANSACTIONS ON CIRCUITS AND SYSTEMS II: ANALOG AND DIGITAL SIGNAL PROCESSING, as well as for the IEEE SIGNAL PROCESSING LETTERS. He received the Charles H. Wilts Prize in 1997 for outstanding independent research in electrical engineering at Caltech.